ACCOUNTS of chemical research

Article

pubs.acs.org/accounts

Raman Spectroscopy and *in Situ* Raman Spectroelectrochemistry of Isotopically Engineered Graphene Systems

Published as part of the Accounts of Chemical Research special issue "2D Nanomaterials beyond Graphene".

Otakar Frank,[†] Mildred S. Dresselhaus,[‡,§] and Martin Kalbac*[,†]

[†]J. Heyrovský Institute of Physical Chemistry of the Academy of Sciences of the Czech Republic, v.v.i., Dolejškova 3, CZ-18223 Prague 8, Czech Republic

[‡]Department of Electrical Engineering and Computer Science, Massachusetts Institute of Technology, Cambridge, Massachusetts 02139, United States

[§]Department of Physics, Massachusetts Institute of Technology, Cambridge, Massachusetts 02139, United States

CONSPECTUS: The special properties of graphene offer immense opportunities for applications to many scientific fields, as well as societal needs, beyond our present imagination. One of the important features of graphene is the relatively simple tunability of its electronic structure, an asset that extends the usability of graphene even further beyond present experience. A direct injection of charge carriers into the conduction or valence bands, that is, doping, represents a viable way of shifting the Fermi level. In particular, electrochemical doping should be the method of choice, when higher doping levels are desired and when a firm control of experimental conditions is needed.

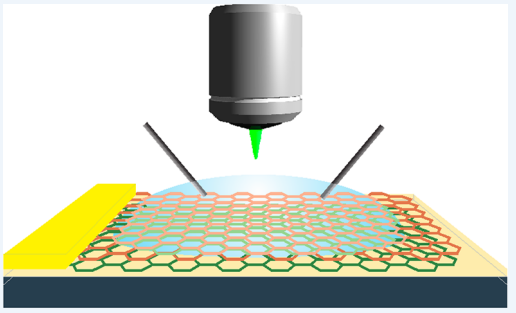

In this Account, we focus on the electrochemistry of graphene in combination with *in situ* Raman spectroscopy, that is, *in situ* Raman spectroelectrochemistry. Such a combination of methods is indeed very powerful, since Raman spectroscopy not only can readily monitor the changes in the doping level but also can give information on eventual stress or disorder in the material. However, when Raman spectroscopy is employed, one of its main strengths lies in the utilization of isotope engineering during the chemical vapor deposition (CVD) growth of the graphene samples. The *in situ* Raman spectroelectrochemical study of multilayered systems with smartly designed isotope compositions in individual layers can provide a plethora of knowledge about the mutual interactions (i) between the graphene layers themselves, (ii) between graphene layers and their directly adjacent environment (e.g., substrate or electrolyte), and (iii) between graphene layers and their extended environment, which is separated from the layer by a certain number of additional graphene layers. In this Account, we show a few examples of such studies, from monolayer to two-layer and three-layer specimens and considering both turbostratic and AB interlayer ordering. Furthermore, the concept and the method can be extended further beyond the three-layer systems, for example, to heterostructures containing other 2-D materials beyond graphene.

Despite a great deal of important results being unraveled so far through the *in situ* spectroelectrochemistry of graphene based systems, many intriguing challenges still lie immediately ahead. For example, apart from the aforementioned 2-D heterostructures, a substantial effort should be put into a more detailed exploration of misoriented (twisted) bilayer or trilayer graphenes. Marching from the oriented, AB-stacked to AA-stacked, bilayers, every single angular increment of the twist between the layers creates a new system in terms of its electronic properties. Mapping those properties and interlayer interactions dependent on the twist angle represents a sizable task, yet the reward might be the path toward the realization of various types of advanced devices.

And last but not least, understanding the electrochemistry of graphene paves the way toward a controlled and targeted functionalization of graphene through redox reactions, especially when equipped with the possibility of an instantaneous monitoring of the thus introduced changes to the electronic structure of the system.

INTRODUCTION

Graphene is a popular material due to its special and unique properties that are encouraging for numerous applications in nanodevices. However, the up-and-coming utilization of graphene necessitates a deeper comprehension of its electric and electronic properties in its neutral and charged states. The tunability of graphene optical and transport properties realized by a shift of the Fermi level, by adding carriers to either the conduction or valence bands represents one of big advantages of this unique material. Hence, the ability to shift the Fermi

Special Issue: 2D Nanomaterials beyond Graphene

Received: October 20, 2014
Published: January 8, 2015

DOI: 10.1021/ar500384p
Acc. Chem. Res. 2015, 48, 111−118

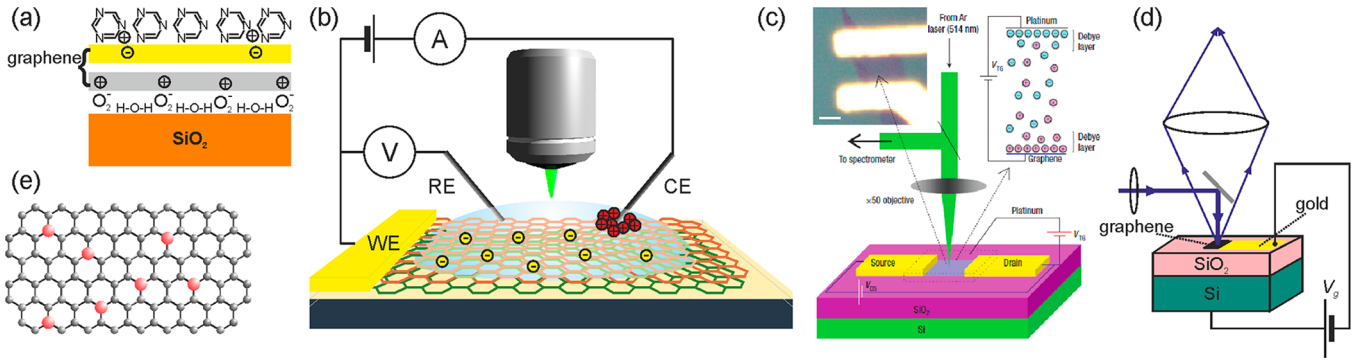

Figure 1. Sketches of different doping experiments conducted on graphene: (a) chemical doping (adapted with permission from ref 1), (b) electrochemical three-electrode setup used, for example, in refs 3 and 5, (c) electrochemical gating setup (reprinted with permission from ref 2, copyright 2008 Nature Publishing Group), (d) electrostatic gating setup (adapted with permission from ref 7, copyright 2007 American Physical Society), and (e) incorporation of atoms into the graphene lattice.

level presents a vital degree of freedom augmenting the range of potential applications of this exceptional material.

In general, graphene can be doped chemically (also called molecular doping),[1] electrochemically,[2−5] by electrostatic gating,[6,7] or by a direct introduction of heteroatoms into the lattice, see Figure 1.[8] Till now, such experiments on graphene have usually been performed using electrochemical or electrostatic doping since these methods provide a direct approach to manipulate the Fermi level of graphene.[2−5,7,9−11] Electrostatic backgating[7,12] is used for its simplicity and a straight application channel to field-effect transistors,[13] but it has several downsides. First, electrostatic gating relies on the dielectric layer properties. Because the efficiency of doping is commonly modest and therefore a relatively high voltage needs to be applied, the accessible magnitude of doping levels is restricted. For example, Yan et al.[7] used a gate voltage range of −80 to 80 V to reach carrier densities from (8 to −4) × 10^{12} cm^{-1}. Additionally, a high applied voltage can cause charge trapping by the substrate, thereby altering its properties. The experimental results are then more challenging to interpret and to reproduce from one sample to another. In contrast, electrochemical doping is efficient, in that an electrode potential of ±1.5 V suffices for typical experiments, thereby reaching carrier concentrations of approximately ±5 × 10^{13} cm^{-2}.[3,5,9] However, further extension of the doping range is highly desirable and can be achieved using liquid electrolyte in conjunction with a protective layer.[14,15] In a standard electrochemical experiment, the complications with charge trapping are mitigated, because the carriers are transferred to the sample through an ohmic contact and recompensated by an electrolyte counterion. Moreover, graphene responds to electrochemical doping quickly enough, and thus the measurement speed is generally hampered only by the time required to get sufficient intensity of the signal in the spectrum. On the other hand, the electrochemical method demands distinct cell geometry, high chemical purity of the electrolyte salt and solvent, and high quality electrodes.[16] Furthermore, a three electrode setup with a reference electrode (apart from the counter and working electrodes) has to be utilized to precisely control the applied voltage.[17]

Before the rise of graphene,[18] the *in situ* combination of Raman spectroscopy with electrochemistry, that is, Raman spectroelectrochemistry, had already proven useful for the study of fullerenes and carbon nanotubes.[16] The important features monitored in the Raman spectra of pristine graphene (Figure 2) are the symmetry-allowed G and G′ modes[19,20] (the

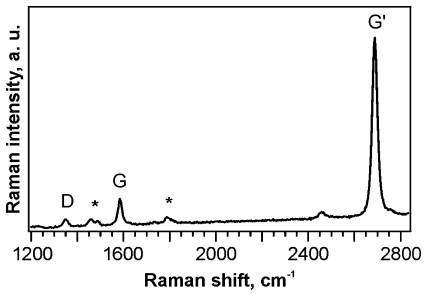

Figure 2. Raman spectrum of single-layer CVD graphene at 0 V, excited by 2.33 eV laser excitation energy, in an electrochemical environment. Raman bands of the electrolyte are indicated by asterisks. Reprinted with permission from ref 5. Copyright 2010 American Chemical Society.

latter also termed as the 2D mode[19]). They can be found in the Raman spectra of other graphene-derived materials, but their particular Raman shifts, line-widths, and intensities are affected by the laser excitation energy, number of graphene layers, doping, strain, etc.[6,21] The D line can also appear in Raman spectra of some graphene samples indicating the presence of symmetry-breaking perturbations. A few recent studies describe the spectroelectrochemical behavior of the D band in graphene,[22−24] showing the tunability of the D peak presence (both reversibly and irreversibly)[23,24] but also its response to the applied potential.[22]

For fundamental research, mechanically cleaved graphene[18] has usually been favored over CVD graphene[25] mostly owing to the lower quality of CVD graphene in the early stages of its development. However, with the recent rapid progress in both CVD growth (graphene domains with sizes over 1 mm^2 now available[26]), and the consecutive graphene transfer, the quality contrast between the samples has become smaller. On top of that, CVD growth provides one special tool inaccessible by mechanical cleavage, namely, that of carbon isotope labeling,[27] which is the focus of this Account. Thus, CVD-prepared graphene significantly simplifies sample processing, thereby facilitating more detailed studies with such samples.

Since CVD graphene is of high current interest, we discuss in this Account the electrochemical results obtained thus far when using CVD graphene. Although these results are similar to those obtained on cleaved graphene samples, one should expect some minor differences due to the grain boundaries and wrinkles or folds that are more common in CVD graphene.

DOI: 10.1021/ar500384p
Acc. Chem. Res. 2015, 48, 111−118

This Account will successively describe the cases of monolayer graphene (referred to as 1-LG), sequentially transferred two- and three-layer graphene (2-LG and 3-LG, respectively), and bilayer graphene grown in one step (AB 2-LG or turbostratic 2-LG, depending on the relative crystallographic orientation between the two layers).

MONOLAYER GRAPHENE

In general, the G band frequency shift in doped graphene is governed by the alterations of the C−C bond strength and by the phonon energy renormalization.[28] In graphene, the similarity of time scales of electron and phonon dynamics allows a coupling between lattice vibrations and Dirac fermions. Therefore, description of the G band phonons by the adiabatic Born−Oppenheimer approximation is not appropriate,[19,28] and time-dependent perturbation theory is used instead. In this description, an electron is first excited from the valence band (referred to as π) to a conduction band (π^*) by absorbing a phonon, and an electron−hole pair is thus created. The electron and the hole then recombine and emit a phonon, whose lifetime and frequency are now notably altered by this second-order process.[6] As a consequence, the energies of both the phonons and the carriers are renormalized. In doped graphene, the creation of electron−hole pairs can be quenched, as the Fermi energy, E_F, is shifted from the Dirac point.[28] The change of the G band frequency is expected to be the same for positive and negative doping because of electron−hole symmetry. However, the C−C bond strength is also influenced by doping.[7] Electrons are removed from antibonding orbitals upon positive doping, which results in a hardening of the G mode. Conversely, electrons are added to the antibonding orbitals upon negative doping, and therefore Raman G mode frequency (ω_G) downshift is expected, as is known from the studies of graphite intercalation compounds.[29]

In graphene, the effects of both renormalization of the phonon energy and change of the C−C bond strength are superimposed in the experimental data. For positive charging, the two effects add up resulting in an upshift of ω_G.[2,5] In contrast, these effects result in an opposite sign of the G band frequency shift during negative charging.[2,5] These arguments are in line with the electrochemical experiments, where ω_G was found to rise monotonically at positive electrode potentials and nonmonotonically at negative potentials.[2] Additionally, the measured shift never becomes as high for negative doping as it does for positive doping.[5]

As discussed above, the evolution of the Raman G and G′ modes upon electrochemical doping has been first examined for mechanically cleaved graphene samples.[2] The obtained data are fully comparable to the results gathered for the CVD graphene,[5] verifying that the electronic structure of graphene is tunable independently of its preparation method. Nevertheless, it should be noted that different authors may use different electrolytes and also different electrochemical set-ups, and these differences explain some of the inconsistencies between the published results that were observed by different research groups. More specifically, the doping efficiency can often be such an issue. Hence, much higher electrode potentials were needed in the case of less efficient electrolytes[2] to achieve the same effect as in the case of highly efficient electrolytes.[14]

In spectroelectrochemistry measurements,[16] when a high electrochemical potential is needed, nonaqueous electrolytes are preferred over the aqueous ones due to the early onset of water decomposition at both positive and negative potentials, giving a limited potential window of less than 2 V for the electrochemical study of turbostratic sp^2 materials.[24] If allowed by the sample conditions, that is, by a good adhesion to the substrate, a liquid electrolyte is advantageous due to a generally better conductivity compared with polymer-based electrolytes.

An example be given for electron doping, where in ref 5 an electrode potential of −1.2 V caused the maximum Raman G band shift of 1604 cm^{-1} (Figure 3, left), whereas an electrode potential of about −4 V was needed to attain the same ω_G in an earlier work.[2] It has to be mentioned that common electrolytes start to undergo irreversible changes at potentials much lower than −4 V. Consequently, this means that measurements conducted at such potentials were probably not carried out under an equilibrium state and the polarization of the graphene working electrode was not perfectly quantitative from an electrochemical standpoint. Obtaining a high doping efficiency is thus essential for proper analysis of the electrochemical data collected at larger doping levels, because electrolyte or electrode instabilities may take place at high potentials and such high potentials need to be avoided for obtaining reproducible results.

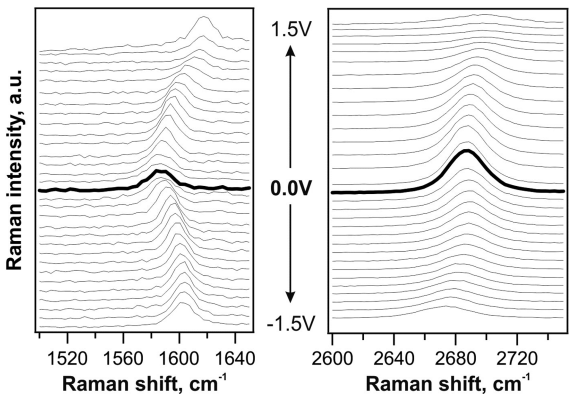

Figure 3. *In situ* Raman spectroelectrochemical data for ω_G (left) and $\omega_{G'}$ (right) on 1-LG. The separation between traces is 0.1 V. The spectra are excited by 2.33 eV laser radiation. Adapted with permission from ref 5. Copyright 2010 American Chemical Society.

We also note that throughout this Account, the potentials refer to the graphene working electrode. Therefore, hole doping is denoted by positive potential values and electron doping by negative values. Such a convention is customary in electrochemical works.[3−5,16] That is in contrast to some works, where the potentials values refer to the reference (gate) electrode.[2,10,11] Such notation gives the opposite sign to the potential values, compared with conventional electrochemistry. Hence, in this other non-conventional case, hole doping of graphene is denoted by negative potential values, while electron doping of graphene is denoted by positive electrode potentials values. Thus, when considering electrochemical measurements of graphene, it is important for authors to define the signs corresponding to electron and hole doping and for the reader to be aware of possible differences in notations between one report and another.

The Raman G′ mode frequency ($\omega_{G'}$) reacts sensitively to doping as well but differently than the G mode (Figure 3, right). Increasing the magnitude of the positive potentials results in an increase of $\omega_{G'}$, while at negative potentials $\omega_{G'}$ increases slightly at first, followed by a rather large downshift in frequency. In the range of 0−1 V, the potential-dependent

DOI: 10.1021/ar500384p
Acc. Chem. Res. 2015, 48, 111−118

change of the G′ mode frequency exhibits a slope of $\Delta\omega_{G'}/\Delta V$ = 9 cm^{-1}/V, while the G mode slope in the same potential range was $\Delta\omega_G/\Delta V$ = 18 cm^{-1}/V.[5] The ratio between $\Delta\omega_{G'}/\Delta V$ and $\Delta\omega_G/\Delta V$ gives 0.5, which corresponds very well with theoretical prediction.[30] The change of $\omega_{G'}$ upon doping arises from the effects of variations of the electron−electron interactions, electron−phonon coupling, and C−C bond strength. It should be noted that the distinct mutual changes of $\Delta\omega_G$ vs $\Delta\omega_{G'}$ induced by doping and strain can be used to disentangle these two effects in graphene under various conditions, such as the conditions caused by (i) varying the interaction between CVD graphene and underlying copper single crystals,[31] (ii) modifying the interface between exfoliated graphene and the Si/SiO_2 substrate,[32] or (iii) back-gating epitaxial graphene on SiC.[33]

The intensities (areas) of both the G and G′ Raman modes for graphene manifest a considerable and mode-specific evolution in response to the electrode potential. The most notable effect, which appears at potentials over +1.0 V, is an extreme enhancement of the intensity of the Raman G band (Figure 4 top). This intensity increase depends sensitively on

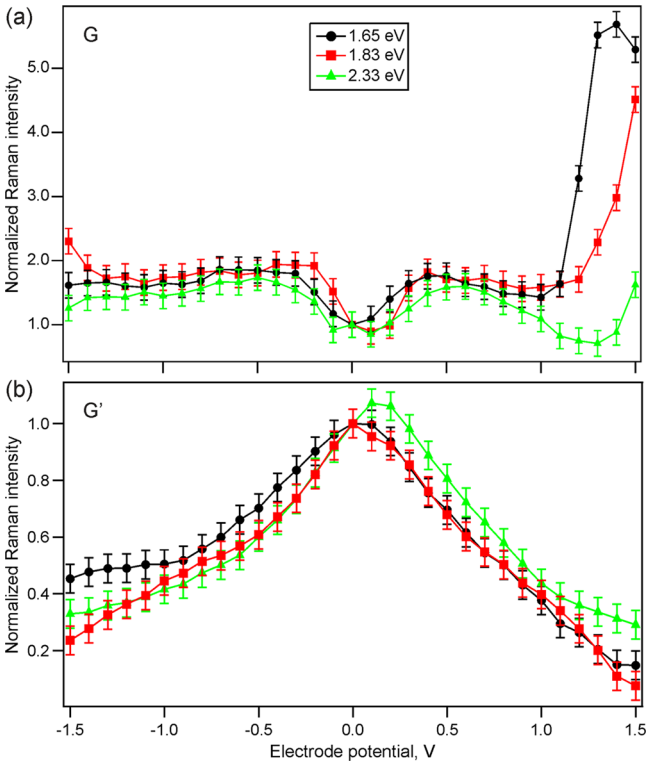

Figure 4. Dependence of the Raman intensity on electrode potential for the (a) G and (b) G′ modes at various laser excitation energies. Reprinted with permission from ref 5. Copyright 2010 American Chemical Society.

the laser excitation energy, where it was strongest and with the earliest onset for the lowest excitation energy used (1.65 eV).[5]

In "neutral" graphene, the phonons can dissipate energy through the creation of an electron−hole pair.[28,30] In charged graphene such a process is quenched since the end state is either empty (for hole doping) or occupied (for electron doping), which causes narrowing of the G band.[7,28,30] After the removal of the Kohn anomaly,[5] the intensity of the G band does not change upon further electron doping and up to 1.0 V for hole doping, in agreement with previous calculations and experimental results.[7] However, a similar increase of the signal intensity at high positive potentials was also observed in an experiment using an ionic liquid electrolyte.[34] Such appearance of the dramatic intensity increase is in accordance with theoretical work by Basko.[35] When the Fermi level approaches $E_{laser}/2$, the G band matrix element should increase.[35] Additionally, the Fermi level will reach the value of $E_{laser}/2$ at a smaller positive potential when a smaller laser excitation energy is used. The excitation energy dependence of the enhancement observed in Figure 4 clearly corresponds to the latter case.

The Raman G′ band intensity monotonically decreases for both doping directions, yet at slightly different rates (Figure 4, bottom).[5] Basko et al. proposed a proportionality between the G′ band intensity and the electron/hole inelastic scattering rate.[36] Since the charging increases the number of carriers, the chance of a scattering event increases too, which should cause the observed decrease of the Raman G′ band intensity.

TWO- AND THREE-LAYER GRAPHENE

Controlling and manipulating the doping of individual graphene layers in few layer graphene samples remains a major challenge in graphene research. Probing the doping state of individual layers can be realized by a new concept which combines Raman spectroscopy and isotope labeling. The isotope labeling approach allows an experimentalist to prepare individual graphene layers with distinct content for each carbon isotope.[27] We review here the results obtained on 2-LG[3] and 3-LG[4], but the same approach may be used for even higher numbers of graphene layers.

Figure 5 shows an example of Raman spectra measured *in situ* on an electrochemically doped 2-LG sample in which the bottom layer (in contact with SiO_2) was graphene containing predominantly the ^{12}C isotope (i.e., the natural isotope composition) and the top-layer contained 99% ^{13}C isotope (i.e., the purity of the purchased chemical). In both layers, the

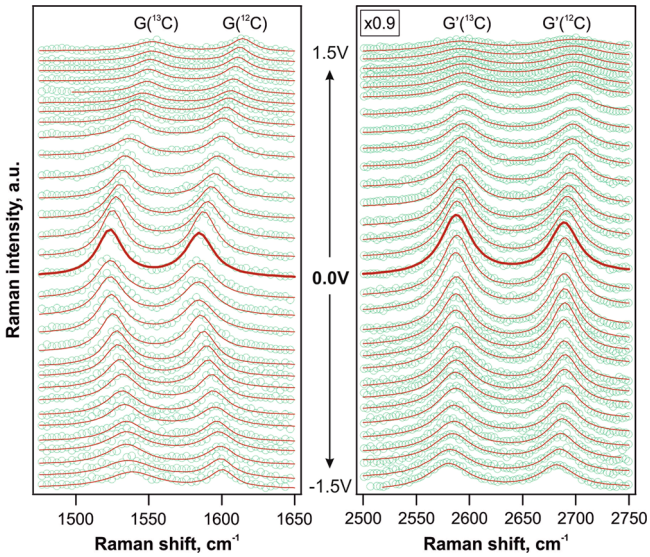

Figure 5. *In situ* Raman spectroelectrochemical data for ω_G (left) and $\omega_{G'}$ (right) of a 2-LG sample. The circles represent the experimental points, and the solid line is their fit with a Lorentzian line shape. The spectra are excited by 2.33 eV laser excitation energy. Adapted with permission from ref 3. Copyright 2011 American Chemical Society.

DOI: 10.1021/ar500384p
Acc. Chem. Res. 2015, 48, 111−118

frequencies and intensities of the Raman G and G′ features vary significantly with the changes of electrode potential,[3] as can be seen in Figure 5.

The G band is upshifted by 32−33 cm^{-1} at +1.5 V both for the ^{12}C bottom layer and the ^{13}C top layer and by 17 cm^{-1} at −1.5 V, again, regardless of the layer position. Over the same potential range, the G′ mode upshifts by 9 cm^{-1} at positive potential and downshifts by 5−6 cm^{-1} at negative potential, regardless of the layer. Hence, it is obvious that the evolution of both the G band and the G′ band with applied positive and negative potentials is alike for both the top and bottom layer of 2-LG samples.

The same electrode potential dependence of ω_G and $\omega_{G'}$ for the ^{13}C and the ^{12}C layers in the 2-LG under study points to an equal charge accumulated on the two layers at each particular potential.[3] It should be noted that both graphene layers are in ohmic contact but only the top layer is in the direct contact with the electrolyte. Counterions from the electrolyte thus have to compensate the charge on the bottom graphene layer through the top layer. The identical evolution of the doped bottom and top layers in 2-LG suggests only a weak influence by the electrolyte. In other words, solely the alterations caused by the electric field are manifested in the behavior of the bottom layer, while, apart from the electric field, the top layer is affected also by the double layer formed at the graphene/electrolyte interface. Note that there is no indication of Li^+ intercalation between the layers, not even at the lowest potential of −1.5 V.

The G and G′ band Raman intensities in the 2-LG are reduced as the potential magnitude is increased for both doping directions, in a similar fashion for the top and the bottom layer.[3] There is no visible stacking order of the two graphene layers, and therefore no or only minor coupling between the layers could be expected, in contrast to AB-stacked bilayers (see below). Hence, the individual layers in the 2-LG should behave as they do in 1-LG under electrochemical doping. However, that is obviously not the case, especially as far as the G mode intensity is concerned, where substantial differences can be observed.[3,5] The unexpected G mode intensity drop in the case of the 2-LG sample might be caused by Coulomb repulsion of the two layers. As shown in recent works, the interaction between misoriented layers of graphene can result in the emergence of Van Hove singularities in the electronic states or in a leveling out of the electronic bands at certain angles of misorientation, dependent on the laser excitation energy.[37−40] In analogy to the general case studied above, one can expect that the decoupling of the layers through doping can revert the electronic structure and thereby quench any enhancement effects caused by the interlayer interactions. Indeed, a gradual cancellation of the G band enhancement in bilayers twisted by the critical angle was observed *in situ* during an electrostatic gating experiment.[41] On the other hand, no changes in the G band intensity were observed in bilayers twisted by an angle deviating far from the critical angle. Variations in the 2D band (appearance or disappearance of an additional $2D^+$ component) upon charging were observed in the same experiment.[41]

In the case of 3-LG, the combination of isotopically pure graphene layers is not sufficient to distinguish individual graphene layers. A mixing of isotopes is needed to achieve a shift of the Raman modes to a suitable frequency between the peaks of original ^{13}C and ^{12}C graphene.[4] The straightforward case is the 3-LG assembly composed of layers of natural ^{12}C graphene on top, a 1:1 mixture of $^{12}C/^{13}C$ in the middle, and pure ^{13}C graphene at the bottom, see Figure 6. By a combination of these three randomly stacked monolayers, 3-LG can be retrieved. The frequencies of the Raman modes in the specially stacked layers are found to be shifted with respect to those of 1-LG. The variations in frequency shifts may be linked to the variations in doping,[5] stress,[42] and interlayer interactions,[40] and these differences evidently vary for each specific layer as they do also from the three monolayers on the substrate. Hence isotopically engineered few layer graphene is an ideal system to explore the influence of the environment and the substrate. The bottom layer in the 3-LG is in contact with the substrate, the top layer with the environment, and the middle one solely with graphene layers on either side.[4]

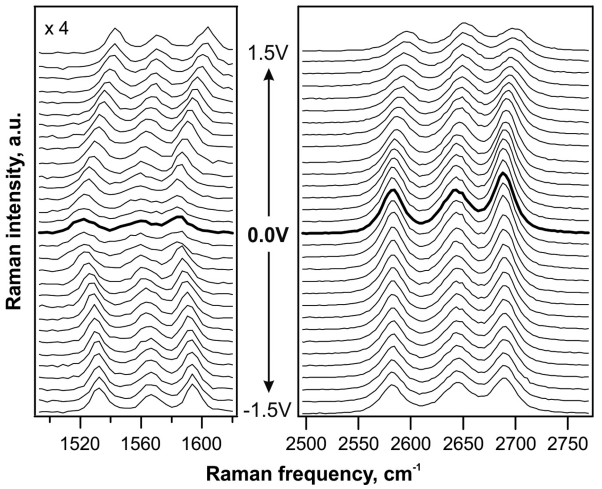

Figure 6. *In situ* Raman spectroelectrochemical data for ω_G (left) and $\omega_{G'}$ (right) of a 3-LG sample, excited by 2.33 eV laser excitation energy. The top layer is ^{12}C, the middle layer is $^{12/13}C$, and the bottom layer is ^{13}C. Adapted with permission from ref 4. Copyright 2012 American Chemical Society.

Figure 6 shows an example of *in situ* Raman spectroelectrochemical measurements taken on 3-LG.[4] Like in the case of 1-LG[5] and 2-LG,[3] the 3-LG[4] Raman features show a notable dependency on the doping. The evolution of Raman spectra of specific layers in 3-LG reflects their position in the stack. In the case of ref 4, all three layers were contacted as the working electrode, but each layer had a particular environment: graphene and substrate for the bottom layer, graphene and graphene for the middle layer, and graphene and electrolyte for the top one. The spectroelectrochemical data show, therefore, the impact of the environment on the evolution of the Raman features during electrochemical doping. Additionally, the influence of the adjacency of electrolyte ions on graphene can be determined from the experimental data. The electrolyte counterions, which compensate the charges injected into the graphene layers are in direct contact only with the top graphene layer. The middle and bottom layers are separated from the electrolyte by one and two layers of graphene, respectively.[4]

The electrode potential influences the Raman features of all three layers in the stack. Hence, the top layer screens neither the middle layer nor the bottom one. Figure 7 shows the middle layer exhibiting an almost model evolution with only a slight asymmetry of the frequency shifts for the hole and electron doping.[4] On top of that, the ω_G fulfills the theoretical predictions at low doping levels:[28] there is a local maximum at 0 V and two local minima between ±0.1−0.2 V, which coincide

DOI: 10.1021/ar500384p
Acc. Chem. Res. 2015, 48, 111−118

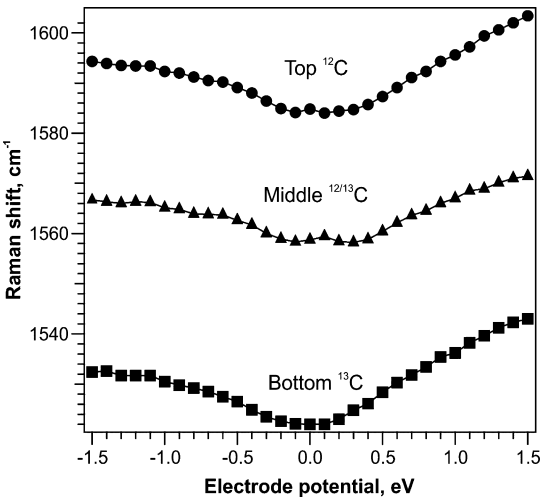

Figure 7. *In situ* Raman spectroelectrochemical data for the G-band of a 3-LG. The spectra are excited by 2.33 eV laser excitation energy. Reprinted with permission from ref 4. Copyright 2012 American Chemical Society.

with the G mode phonon energy. The largest asymmetry for the electron/hole doping is shown for ω_G of the bottom layer (Figure 7), which illustrates an impact of the charges trapped in the SiO_2 support on the directly overlying graphene.[4]

Furthermore, there is no effect resembling the metallic screening of the electrostatic potential of the electrolyte ions in the case of graphene layers. This observation is consistent with the theoretical prediction of Guinea,[43] which proposed that intralayer hopping results in a distribution of charges over many graphene layers.

The preceding results describe the situation in randomly oriented graphene layers, where the turbostratic few-layer graphene can be easily obtained by the subsequent transfer of individual, isotopically labeled layers onto the target substrate.[3,4,27] However, the rotation angle between the graphene layers is difficult to control, and also the sequential transfer routine may introduce impurities between the layers. Hence, it is hardly possible to produce AB-2LG in this way. Recently, numerous works on graphene adlayers (as-grown by the CVD procedure) appeared.[44−46] The adlayers are, in general, multilayer seeds evolved during the deposition of a primary 1-LG using a copper catalyst. AB-stacked regions are often formed in the adlayers. If the isotope composition of the CH_4 precursor and the growth conditions are properly controlled, the continuous layer can be composed of mostly one isotope (either ^{12}C or ^{13}C) and the adlayer consists of the second isotope.[27] Moreover, regions with both AB and turbostratic configurations can be found within the same grains, which allows a comparison to be made between the response of the external perturbations regarding their dependence on the stacking order.[9] In such a specimen, the individual layers can be addressed by Raman spectroscopy to monitor the impact of phonon self-energy renormalizations for each particular layer independently and to deepen the knowledge about the interlayer interactions. The AB 2-LG reveals two separate G modes, designated LG (lower frequency) and HG (higher frequency), due to a mass-related inversion symmetry-breaking.[9] These modes are associated with a symmetric (LG) and an antisymmetric (HG) combination of E_g and E_u modes. Normally, only the E_g is a Raman-active mode in the $^{12/12}C$ AB-stacked 2-LG, where no mass-related symmetry-breaking occurs. In the case of $^{12/13}C$ AB 2-LG, this symmetry is naturally lifted, because of the different isotopes constituting the unit cells in the top layer and the bottom layer. This is different from $^{12/13}C$ turbostratic 2-LG, where the two separate G bands are just linked to the E_g modes from the noninteracting ^{13}C and ^{12}C layers. Electrochemical doping has different effects on the AB and turbostratic 2-LG (Figure 8).[3,9] In the case of the AB 2-LG, the frequency shifts of the LG

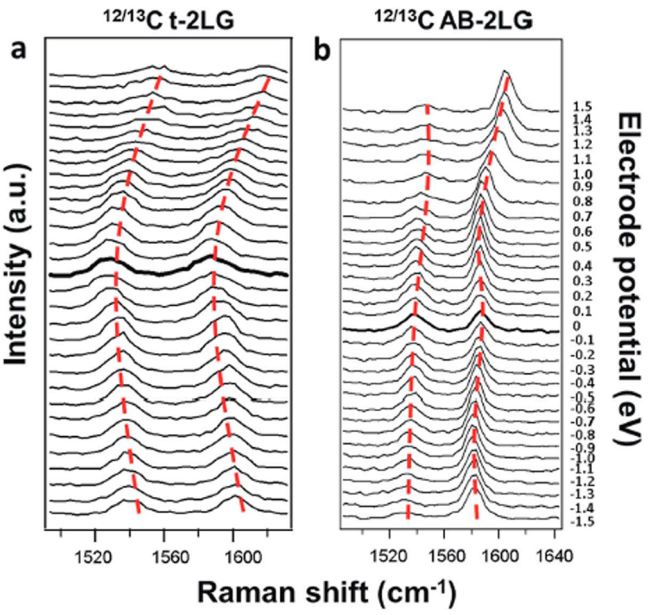

Figure 8. *In situ* Raman spectroelectrochemistry of the G-modes in 12C/13C turbostratic (a) and AB-stacked (b) bilayer graphene, excited by the 2.33 eV laser excitation energy. Reprinted from ref 9. Copyright 2013 Nature Publishing Group.

and HG modes are smaller and more complex, and also the intensity ratio between these two modes shows a distinct and characteristic evolution with the applied potential.[9] An explanation can be proposed by employing the band gap opening as another process involved in the doping of the AB 2-LG. The frequencies of the LG and HG modes decrease for negative potentials in the AB 2-LG, meaning that the variations in the strengths of the C−C bonds are responsible for the observed effects in this potential region. In the AB 2-LG, the electrochemical doping reflects a lesser sensitivity of E_F to the electrode potential because of the distinct electronic structure, in contrast to that for the turbostratic 2-LG. Additionally, spectroelectrochemical data from AB-2LG manifested less charge present on the bottom layer than on the top layer, a situation that is analogous to a device with a fixed potential at the bottom gate (realized through the permanent doping from the silicon substrate) and a variable potential at the top gate (realized electrochemically by varying the applied voltage).[9]

■ CONCLUSIONS

We have shown some of the possibilities of using *in situ* Raman spectroelectrochemistry to study graphene generally and CVD graphene in particular. The use of electrochemical experiments allows researchers to reach higher doping levels together with a better control of the potential through the three-electrode setup, compared with other methods for controlling the Fermi level. One of the most important consequences of the higher applied potentials is the observation of a cancellation of the

DOI: 10.1021/ar500384p
Acc. Chem. Res. 2015, 48, 111−118

interference effects causing a strong increase in intensity of the G band at positive potentials. In particular, lowering the Fermi level to one-half of the excitation photon energy allows more detailed quantitative studies of the effects of electron and hole doping of semiconductors. Furthermore, the employment of isotope labeling in the CVD process opens up other opportunities in addressing individual layers in multilayered systems when carrying out Raman experiments. Electrochemical doping is also shown to allow studies of 2-LG graphene with distinct and different stacking orders, as well as in distinguishing spectroscopically the effects of charging the bottom, middle, or top layers in a 3-LG system.

AUTHOR INFORMATION

Corresponding Author

*Tel: 420 2 6605 3804. Fax: 420 2 8658 2307. E-mail: kalbac@jh-inst.cas.cz.

Funding

The authors (O.F. and M.K.) acknowledge the support of MSMT Project (Grant LH13022), MSMT ERC-CZ Project (Grant LL1301), and European Union FP7 Programme (Grant No. 604391 Graphene Flagship), while M.S.D. acknowledges Grant NSF-DMR 10-04147.

Notes

The authors declare no competing financial interest.

Biographies

Dr. Otakar Frank is a junior group leader within the Department of Electrochemical Materials at J. Heyrovsky Institute of Physical Chemistry of the Academy of Sciences of the Czech Republic in Prague. He obtained his Ph.D. degree in 2005 at the Charles University in Prague. His main research interests include mechanical and electronic properties of graphene and related nanostructures.

Prof. Mildred S. Dresselhaus is an Institute Professor at MIT in the departments of Electrical Engineering and Physics, and has been active in materials research since the 1950s. Recent research activities in the Dresselhaus group that have attracted attention are in the areas of carbon nanotubes, bismuth nanostructures, and low-dimensional thermoelectricity.

Dr. Martin Kalbac graduated in inorganic chemistry from the Charles University, Prague, Czech Republic (1998), where he also received a Ph.D. degree in 2002. Since 2001, he has worked at the J. Heyrovsky Institute of Physical Chemistry of the AS CR in Prague, as a research scientist. From 2010, he has been a vice-director of the institute, and from 2013, he has led the Department of Low Dimensional Systems. His research interest includes spectroscopy and spectroelectrochemistry of carbon nanotubes and graphene.

REFERENCES

(1) Zhang, W.; Lin, C.-T.; Liu, K.-K.; Tite, T.; Su, C.-Y.; Chang, C.-H.; Lee, Y.-H.; Chu, C.-W.; Wei, K.-H.; Kuo, J.-L.; Li, L.-J. Opening an Electrical Band Gap of Bilayer Graphene with Molecular Doping. *ACS Nano* **2011**, *5*, 7517−7524.

(2) Das, A.; Pisana, S.; Chakraborty, B.; Piscanec, S.; Saha, S. K.; Waghmare, U. V.; Novoselov, K. S.; Krishnamurthy, H. R.; Geim, A. K.; Ferrari, A. C.; Sood, A. K. Monitoring Dopants by Raman Scattering in an Electrochemically Top-Gated Graphene Transistor. *Nat. Nanotechnol* **2008**, *3*, 210−215.

(3) Kalbac, M.; Farhat, H.; Kong, J.; Janda, P.; Kavan, L.; Dresselhaus, M. S. Raman Spectroscopy and in Situ Raman Spectroelectrochemistry of Bilayer C-12/C-13 Graphene. *Nano Lett.* **2011**, *11*, 1957−1963.

(4) Kalbac, M.; Kong, J.; Dresselhaus, M. S. Raman Spectroscopy as a Tool to Address Individual Graphene Layers in Few-Layer Graphene. *J. Phys. Chem. C* **2012**, *116*, 19046−19050.

(5) Kalbac, M.; Reina-Cecco, A.; Farhat, H.; Kong, J.; Kavan, L.; Dresselhaus, M. S. The Influence of Strong Electron and Hole Doping on the Raman Intensity of Chemical Vapor-Deposition Graphene. *ACS Nano* **2010**, *4*, 6055−6063.

(6) Malard, L. M.; Pimenta, M. A.; Dresselhaus, G.; Dresselhaus, M. S. Raman Spectroscopy in Graphene. *Phys. Rep* **2009**, *473*, 51−87.

(7) Yan, J.; Zhang, Y. B.; Kim, P.; Pinczuk, A. Electric Field Effect Tuning of Electron-Phonon Coupling in Graphene. *Phys. Rev. Lett.* **2007**, *98*, No. 166802.

(8) Meyer, J. C.; Kurasch, S.; Park, H. J.; Skakalova, V.; Künzel, D.; Groß, A.; Chuvilin, A.; Algara-Siller, G.; Roth, S.; Iwasaki, T.; Starke, U.; Smet, J. H.; Kaiser, U. Experimental Analysis of Charge Redistribution Due to Chemical Bonding by High-Resolution Transmission Electron Microscopy. *Nat. Mater.* **2011**, *10*, 209−215.

(9) Araujo, P. T.; Frank, O.; Mafra, D. L.; Fang, W.; Kong, J.; Dresselhaus, M. S.; Kalbac, M. Mass-Related Inversion Symmetry Breaking and Phonon Self-Energy Renormalization in Isotopically Labeled AB-Stacked Bilayer Graphene. *Sci. Rep* **2013**, *3*, No. 2061.

(10) Das, A.; Chakraborty, B.; Piscanec, S.; Pisana, S.; Sood, A. K.; Ferrari, A. C. Phonon Renormalization in Doped Bilayer Graphene. *Phys. Rev. B* **2009**, *79*, No. 155417.

(11) Chen, F.; Qing, Q.; Xia, J.; Li, J.; Tao, N. Electrochemical Gate-Controlled Charge Transport in Graphene in Ionic Liquid and Aqueous Solution. *J. Am. Chem. Soc.* **2009**, *131*, 9908−9909.

(12) Malard, L. M.; Elias, D. C.; Alves, E. S.; Pimenta, M. A. Observation of Distinct Electron-Phonon Couplings in Gated Bilayer Graphene. *Phys. Rev. Lett.* **2008**, *101*, No. 257401.

(13) Schwierz, F. Graphene Transistors. *Nat. Nanotechnol* **2010**, *5*, 487−496.

(14) Kominkova, Z.; Kalbac, M. Extreme Electrochemical Doping of a Graphene-Polyelectrolyte Heterostructure. *RSC Adv.* **2014**, *4*, 11311−11316.

(15) Komínková, Z.; Kalbáč, M. Raman Spectroscopy of Strongly Doped CVD-Graphene. *Phys. Status Solidi B* **2013**, *250*, 2659−2661.

(16) Kavan, L.; Dunsch, L. Spectroelectrochemistry of Carbon Nanostructures. *ChemPhysChem* **2007**, *8*, 975−998.

(17) Kavan, L.; Kalbáč, M.; Zukalová, M.; Dunsch, L. Comment on "Determination of the Exciton Binding Energy in Single-Walled Carbon Nanotubes". *Phys. Rev. Lett.* **2007**, *98*, No. 019701.

(18) Novoselov, K. S.; Geim, A. K.; Morozov, S. V.; Jiang, D.; Zhang, Y.; Dubonos, S. V.; Grigorieva, I. V.; Firsov, A. A. Electric Field Effect in Atomically Thin Carbon Films. *Science* **2004**, *306*, 666−669.

(19) Ferrari, A. C.; Meyer, J. C.; Scardaci, V.; Casiraghi, C.; Lazzeri, M.; Mauri, F.; Piscanec, S.; Jiang, D.; Novoselov, K. S.; Roth, S.; Geim, A. K. Raman spectrum of graphene and graphene Layers. *Phys. Rev. Lett.* **2006**, *97*, No. 187401.

(20) Thomsen, C.; Reich, S. Double Resonant Raman Scattering in Graphite. *Phys. Rev. Lett.* **2000**, *85*, 5214−5217.

(21) Ferrari, A. C.; Basko, D. M. Raman Spectroscopy As a Versatile Tool for Studying the Properties of Graphene. *Nat. Nanotechnol* **2013**, *8*, 235−246.

(22) Bruna, M.; Ott, A. K.; Ijäs, M.; Yoon, D.; Sassi, U.; Ferrari, A. C. Doping Dependence of the Raman Spectrum of Defected Graphene. *ACS Nano* **2014**, *8*, 7432−7441.

(23) Ott, A.; Verzhbitskiy, I.; Clough, J.; Eckmann, A.; Georgiou, T.; Casiraghi, C. Tunable D Peak in Gated Graphene. *Nano Res.* **2014**, *7*, 338−344.

(24) Bouša, M.; Frank, O.; Jirka, I.; Kavan, L. In Situ Raman Spectroelectrochemistry of Graphene Oxide. *Phys. Status Solidi B* **2013**, *250*, 2662−2667.

(25) Reina, A.; Jia, X.; Ho, J.; Nezich, D.; Son, H.; Bulovic, V.; Dresselhaus, M. S.; Kong, J. Large Area, Few-Layer Graphene Films on Arbitrary Substrates by Chemical Vapor Deposition. *Nano Lett.* **2009**, *9*, 30−35.

(26) Chen, S.; Ji, H.; Chou, H.; Li, Q.; Li, H.; Suk, J. W.; Piner, R.; Liao, L.; Cai, W.; Ruoff, R. S. Millimeter-Size Single-Crystal Graphene

DOI: 10.1021/ar500384p
Acc. Chem. Res. 2015, 48, 111−118

by Suppressing Evaporative Loss of Cu During Low Pressure Chemical Vapor Deposition. *Adv. Mater.* **2013**, *25*, 2062−2065.
(27) Frank, O.; Kavan, L.; Kalbac, M. Carbon Isotope Labelling in Graphene Research. *Nanoscale* **2014**, *6*, 6363−6370.
(28) Lazzeri, M.; Mauri, F. Nonadiabatic Kohn Anomaly in a Doped Graphene Monolayer. *Phys. Rev. Lett.* **2006**, *97*, No. 266407.
(29) Dresselhaus, M. S.; Dresselhaus, G. Intercalation Compounds of Graphite. *Adv. Phys.* **2002**, *51*, 1−186.
(30) Piscanec, S.; Lazzeri, M.; Mauri, F.; Ferrari, A. C.; Robertson, J. Kohn Anomalies and Electron-Phonon Interactions in Graphite. *Phys. Rev. Lett.* **2004**, *93*, No. 185503.
(31) Frank, O.; Vejpravova, J.; Holy, V.; Kavan, L.; Kalbac, M. Interaction between Graphene and Copper Substrate: The Role of Lattice Orientation. *Carbon* **2014**, *68*, 440−451.
(32) Lee, J. E.; Ahn, G.; Shim, J.; Lee, Y. S.; Ryu, S. Optical Separation of Mechanical Strain from Charge Doping in Graphene. *Nat. Commun.* **2012**, *3*, 1024.
(33) Fromm, F.; Wehrfritz, P.; Hundhausen, M.; Seyller, T. Looking behind the Scenes: Raman Spectroscopy of Top-Gated Epitaxial Graphene through the Substrate. *New J. Phys.* **2013**, *15*, No. 113006.
(34) Chen, C.-F.; Park, C.-H.; Boudouris, B. W.; Horng, J.; Geng, B.; Girit, C.; Zettl, A.; Crommie, M. F.; Segalman, R. A.; Louie, S. G.; Wang, F. Controlling Inelastic Light Scattering Quantum Pathways in Graphene. *Nature* **2011**, *471*, 617−620.
(35) Basko, D. M. Calculation of the Raman G Peak Intensity in Monolayer Graphene: Role of Ward Identities. *New J. Phys.* **2009**, *11*, No. 095011.
(36) Basko, D. M.; Piscanec, S.; Ferrari, A. C. Electron-Electron Interactions and Doping Dependence of the Two-Phonon Raman Intensity in Graphene. *Phys. Rev. B* **2009**, *80*, No. 165413.
(37) Kalbac, M.; Frank, O.; Kong, J.; Sanchez-Yamagishi, J.; Watanabe, K.; Taniguchi, T.; Jarillo-Herrero, P.; Dresselhaus, M. S. Large Variations of the Raman Signal in the Spectra of Twisted Bilayer Graphene on a BN Substrate. *J. Phys. Chem. Lett.* **2012**, *3*, 796−799.
(38) Kim, K.; Coh, S.; Tan, L. Z.; Regan, W.; Yuk, J. M.; Chatterjee, E.; Crommie, M. F.; Cohen, M. L.; Louie, S. G.; Zettl, A. Raman Spectroscopy Study of Rotated Double-Layer Graphene: Misorientation-Angle Dependence of Electronic Structure. *Phys. Rev. Lett.* **2012**, *108*, No. 246103.
(39) Li, G.; Luican, A.; Lopes dos Santos, J. M. B.; Castro Neto, A. H.; Reina, A.; Kong, J.; Andrei, E. Y. Observation of Van Hove Singularities in Twisted Graphene Layers. *Nat. Phys.* **2010**, *6*, 109−113.
(40) Jorio, A.; Cançado, L. G. Raman Spectroscopy of Twisted Bilayer Graphene. *Solid State Commun.* **2013**, *175*−*176*, 3−12.
(41) Yeh, C.-H.; Lin, Y.-C.; Chen, Y.-C.; Lu, C.-C.; Liu, Z.; Suenaga, K.; Chiu, P.-W. Gating Electron−Hole Asymmetry in Twisted Bilayer Graphene. *ACS Nano* **2014**, *8*, 6962−6969.
(42) Frank, O.; Tsoukleri, G.; Parthenios, J.; Papagelis, K.; Riaz, I.; Jalil, R.; Novoselov, K. S.; Galiotis, C. Compression Behavior of Single-Layer Graphenes. *ACS Nano* **2010**, *4*, 3131−3138.
(43) Guinea, F. Charge Distribution and Screening in Layered Graphene Systems. *Phys. Rev. B* **2007**, *75*, No. 235433.
(44) Fang, W.; Hsu, A. L.; Caudillo, R.; Song, Y.; Birdwell, A. G.; Zakar, E.; Kalbac, M.; Dubey, M.; Palacios, T.; Dresselhaus, M. S.; Araujo, P. T.; Kong, J. Rapid Identification of Stacking Orientation in Isotopically Labeled Chemical-Vapor Grown Bilayer Graphene by Raman Spectroscopy. *Nano Lett.* **2013**, *13*, 1541−1548.
(45) Liu, L.; Zhou, H.; Cheng, R.; Yu, W. J.; Liu, Y.; Chen, Y.; Shaw, J.; Zhong, X.; Huang, Y.; Duan, X. High-Yield Chemical Vapor Deposition Growth of High-Quality Large-Area AB-Stacked Bilayer Graphene. *ACS Nano* **2012**, *6*, 8241−8249.
(46) Ek-Weis, J.; Costa, S. D.; Frank, O.; Kalbac, M. Growth of Adlayers Studied by Fluorination of Isotopically Engineered Graphene. *Phys. Status Solidi B* **2014**, *251*, 2505−2508.

DOI: 10.1021/ar500384p
Acc. Chem. Res. 2015, 48, 111−118